Available online at www.sciencedirect.com

ScienceDirect

Natural Gas Industry B 3 (2016) 173−180

www.elsevier.com/locate/ngib

Research article

Prediction of water formation temperature in natural gas dehydrators using radial basis function (RBF) neural networks

Afshin Tatar[a], Ali Barati-Harooni[b], Hossein Moslehi[c], Saeid Naseri[b], Meysam Bahadori[d], Moonyong Lee[e], Alireza Bahadori[f,*], Adel Najafi-Marghmaleki[b]

[a] *Young Researchers and Elite Club, North Tehran Branch, Islamic Azad University, Tehran, Iran*
[b] *Department of Petroleum Engineering, Ahwaz Faculty of Petroleum Engineering, Petroleum University of Technology (PUT), Ahwaz, Iran*
[c] *Department of Chemical Engineering, Amirkabir University of Technology, Tehran Polytechnic, No. 424, Hafez Avenue, 15875-4413, Tehran, Iran*
[d] *National Iranian Drilling Company, Department of Waste Management, Ahwaz, Iran*
[e] *School of Chemical Engineering, Yeungnam University, Gyeungsan, Republic of Korea*
[f] *Southern Cross University, School of Environment, Science and Engineering, Lismore, NSW, Australia*

Received 22 December 2015; accepted 27 June 2016
Available online 17 August 2016

Abstract

Raw natural gases usually contain water. It is very important to remove the water from these gases through dehydration processes due to economic reasons and safety considerations. One of the most important methods for water removal from these gases is using dehydration units which use Triethylene glycol (TEG). The TEG concentration at which all water is removed and dew point characteristics of mixture are two important parameters, which should be taken into account in TEG dehydration system. Hence, developing a reliable and accurate model to predict the performance of such a system seems to be very important in gas engineering operations. This study highlights the use of intelligent modeling techniques such as Multilayer perceptron (MLP) and Radial Basis Function Neural Network (RBF-ANN) to predict the equilibrium water dew point in a stream of natural gas based on the TEG concentration of stream and contractor temperature. Literature data set used in this study covers temperatures from 10 °C to 80 °C and TEG concentrations from 90.000% to 99.999%. Results showed that both models are accurate in prediction of experimental data and the MLP model gives more accurate predictions compared to RBF model.
© 2016 Sichuan Petroleum Administration. Production and hosting by Elsevier B.V. This is an open access article under the CC BY-NC-ND license (http://creativecommons.org/licenses/by-nc-nd/4.0/).

Keywords: Gas dehydration; Triethylene glycol; Water dew point; MLP; RBF

1. Introduction

Water vapor inevitably accompanies the natural gas, which is extracted from hydrocarbon reservoirs. The existence of water vapor in natural gas, various problems can happen when the natural gas is processed or transmitted. Water vapor present in natural gas can form gas hydrates and plug the line of transmission, form free water, and decrease the capacity of line, corrode the lines of pipes, and reduce the heating value of natural gas. As a result, dehydration is considered as a crucial task in natural gas industry [1]. Several strategies can be adopted to dehydrate natural gas. Considering the needed dehydration specification, either a liquid desiccant or a solid one can be applied, although liquid desiccant is economically more desirable [2]. Glycol, a liquid desiccant, is deemed as the most typical desiccant in dehydration process of natural gas in which dew point depressions in the range of (15−49 °C) are needed [3].

Triethylene glycol (TEG) is the most typical desiccant to dehydrate the natural gas, which is utilized in gas industry. To provide the needed amount of water in the gas exiting from the

* Corresponding author.
E-mail addresses: Afshin.Tatar@gmail.com (Afshin T.), alireza.bahadori@scu.edu.au (Alireza B.).
Peer review under responsibility of Sichuan Petroleum Administration.

http://dx.doi.org/10.1016/j.ngib.2016.06.002
2352-8540/© 2016 Sichuan Petroleum Administration. Production and hosting by Elsevier B.V. This is an open access article under the CC BY-NC-ND license (http://creativecommons.org/licenses/by-nc-nd/4.0/).

contactor, a mass transfer operation is utilized in a counter-current way inside a contactor [4]. A typical TEG system is depicted in Fig. 1. A contactor, a regenerator, a flash tank, and heat exchangers commonly constitute the units of glycol dehydration. Top of the contactor is the entrance of lean TEG liquid stream. On the other hand, bottom of the contactor is where the stream of the natural gas containing water enters. Moving toward the bottom of the contactor, the lean TEG liquid adsorbs the water. Above the contactor, the water-free gas exits. The TEG containing water is directed to the regenerator, where the elimination of water from the rich TEG occurs and then the lean TEG liquid is sent to the contactor [5]. Determination of the minimum amount of TEG to satisfy the water dew point of the gas exiting the contactor has been of great significance in TEG systems. In fact, the amount of TEG concentration is a factor, which plays a prominent role in dew point depression [6]. Consequently, acquiring accurate knowledge about this subject is crucial. Several researches have conducted studies regarding water dew point of natural gas when it is in equilibrium with TEG dehydration.

Because of low concentration of water in the natural gas and high concentration of TEG in the lean TEG stream, TEG solutions with high concentration, more than 99.5 wt.%, are typically needed if the effluent gas stream is required to possess very low concentration of water. As a result, providing equilibrium data with high precision for TEG-water, especially for dilute range of water, is important to precisely design a dehydration unit. Parrish et al. [7] extensively investigated the available equilibrium data and reported that the data presented by Herskowitz and Gottlieb [8] is the most accurate one. Measurement of the activity coefficients of water in TEG was carried out by Herskowitz and Gottlieb [8] at two temperatures of 297.6 K and 332.6 K. In their study, the lowest mole fraction of water was 0.1938 and 0.2961 at respective temperatures of 297.6 K and 332.6 K. They used the van Laar equation to fit the measured activity coefficients. The data for infinite dilution range was not reported in their research. In most researches, extrapolation method was utilized to find

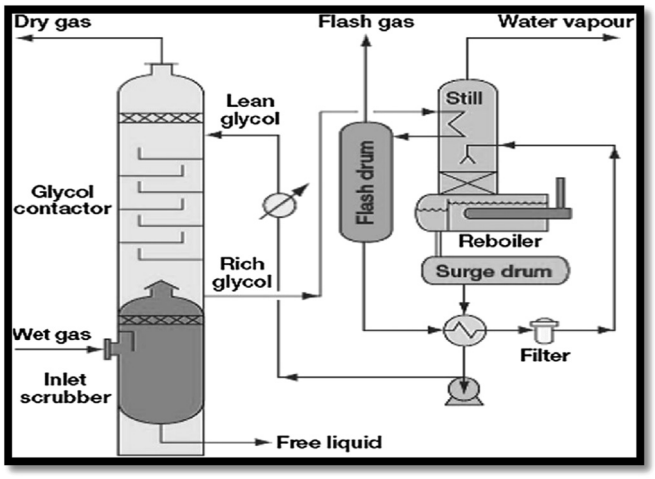

Fig. 1. Typical TEG-Natural gas dehydration system [4].

information about infinite dilution employing a model of activity coefficient like van Laar to describe the infinite dilution range. However, using activity coefficient model causes incorrect outcomes for the infinite dilution activity coefficients. Activity coefficients at infinite dilution as a function of temperature was reported by Parrish et al. [7] for better delineation of the TEG-water system. The data reported by Herskowitz and Gottlieb [8] was in good consistency with the measured infinite dilution activity coefficient data.

Rosman [9] conducted experimental researches to find precise design data for gas−liquid equilibrium in the water-TEG-methane settings. Equilibrium data, which were measured for high concentrations of TEG differ slightly, however the measured values varied noticeably with the rise of equilibrium temperature and water concentration in the TEG, which was in contact with wet gas. He also presented a correlation to extend the results of the study to other pressures and temperatures [9]. Bestani and Shing [10] utilized the gas−liquid partition chromatography approach to measure the activity coefficients of water in TEG, polyethylene glycol (PEG), glycerol, and some mixtures at infinite dilution. They compared the use of these solvents to dehydrate the natural gas at high temperatures. In addition, they proposed a correlation for the corresponding pure solvents which they used in their study on the basis of weight fraction weighted average of data. Scauzillo [11] analyzed different published data and the relevant correlations employing the thermodynamic equilibrium ratio to present equilibrium data that can be utilized to design and assess the glycol dehydration units. The equilibrium ratios of water were employed to solve the glycol contactor problem. He obtained activity coefficients for a system containing different ratios of water in equilibrium with TEG and natural gas and computed the equilibrium dew points for aqueous TEG concentrations in the range of (60−99.9) wt.% and temperature range of (40−120) °F. He presented a correlation to compute the water content in equilibrium with TEG and natural gas, which is applicable to the temperature range of (40−120) °F and for any concentration of TEG.

Bahadori and Vuthaluru [12] presented a model to prognosticate the T_d values in a mixture of stream of natural gas and TEG solution. The input parameters were the amount of TEG in solution and the contractor temperature. Twu et al. [13] utilized the Twu−Sim−Tassone equation of state [14] to determine the phase behavior in a water-TEG system. They also proposed a method to use the Twu−Sim−Tassone equation of state [14] to determine water content and water dew point. The aforementioned studies, Bahadori and Vuthaluru [12] and Twu et al. [13], are good at estimation of parameters but their capability are restricted to the system, which they have been adjusted for. As a result, more researches should be carried out to eliminate such limitations. Recently, artificial neural networks (ANNs), which avoid some difficulties associated with thermodynamic models, have gained attention among various researchers to predict several parameters in petroleum science [15−22]. Regarding TEG dehydration system, Ahmadi et al. [1] used ANN to prognosticate the T_d data in a stream of natural gas by using a TEG solution at

various temperatures and TEG concentrations. Their results showed an acceptable consistency with actual data. Although this ANN model indicated good estimation, other studies can be conducted to improve the precision of the model. As a result, in this study, two intelligent based methods namely MLP and RBF models were implemented for estimation of the experimental T_d values based on the TEG concentration and contractor temperature. Result showed that the developed models could predict the experimental data with an acceptable accuracy. In addition, comparison between two models showed the superiority of MLP model over RBF model. Comparison between published models in literature and models developed in this model showed that the MLP model is more effective and accurate than other models.

2. Details of intelligent model

2.1. Multilayer perceptron (MLP)

Multilayer perceptron (MLP) is one of the most conventional modeling techniques. MLP is a member of a general form of Neural Networks (NN), namely feed-forward NN [23]. Generally, MPLs have three layers in their structure which are input, hidden, and output layers. Each MLP comprises of one or several hidden layers. These hidden layers are composed of several neurons. The neurons of input and output layers are the same as the number of input and output parameters of model [24]. In MLP all neurons (except those neurons which are located in input layer) obtain and train their feed from other neurons [1]. Fig. 2 represents the procedure of information handling by neurons, which are located in hidden layer. According to this figure, which shows a 3-layer feed-forward NN, the input parameters to the 3th hidden neuron are denoted by a_1, a_2, a_3,…,a_m. All of these parameters could be collected in as a single vector. An appropriate weight factor (i.e., $w^H_{3,2}$, $w^H_{3,3}$,…, $w^H_{3,m}$) is multiplied to each input parameter. This multiplication shows the synaptic neural connections by natural nets, which affects the input signs to the neuron by increasing or decreasing their values. These weight factors also help to characterize the strength of input signs because they are tunable constants inside the network. The multiplied and weighted inputs are transferred to summation blocks, which are shown by Σ symbol. There is also a term named bias, b^H_3, for each neuron, which is added to the inputs which are multiplied by related weights to generate the total input of model [15]. A bias is a term, which is has a specific sign and is applied to the neuron; the bias terms have no role in linking the input of a neuron to the output of another neuron. The performance of bias terms in allocating a specific amount of output signs is independent to the sign of inputs. The mathematical expressions for the process of weighting inputs by weight and bias factors are as follows [15]:

$$S^H_3 = NET = \sum_{j=1}^{m} w^H_{3,j} \cdot a_j + b^H_3 \tag{1}$$

Here, the neuron behaves like a transfer function or a neuron activation function by mapping or activating to create an outcome O^H_3 according to the below relationship [1]:

$$O^H_3 = \varphi(NET) = \varphi\left(\sum_{j=1}^{m} w^H_{3,j} \cdot a_j + b^H_3\right) \tag{2}$$

where φ denotes the transfer or activation function. There are various types of transfer functions among which the followings are three general and popular types of these functions:

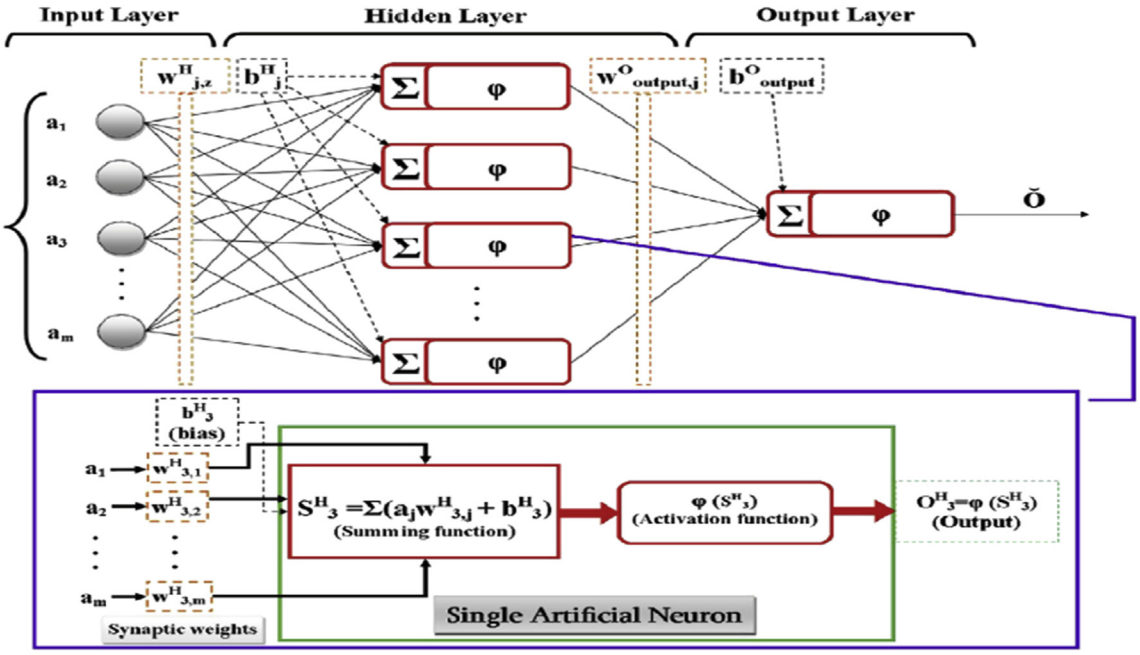

Fig. 2. Schematic of an artificial neuron within the hidden layer in a 3 layer feed-forward neural network [1].

- Log-Sigmoid function (*logsig*)

$$\varphi(s) = \frac{1}{1+e^{-s}} \tag{3}$$

- Hyperbolic tangent function (*tansig*)

$$\varphi(s) = \frac{e^{s}-e^{-s}}{e^{s}+e^{-s}} \tag{4}$$

- Linear function (*purelin*)

$$\varphi(s) = s \tag{5}$$

In MLP, both try and error or intelligent approaches can be used to determine how many hidden layers are required. In addition, these approaches can be used to determine the corresponding neurons in hidden layers to obtain the optimum condition for design of model. The optimum condition of the developed network depends on the Mean Square Error (MSE) of data, which is formulated as below:

$$\mathrm{MSE} = \frac{1}{K}\sum_{l=1}^{K}(Y_l^{\exp} - Y_l^{\mathrm{pre}})^2 \tag{6}$$

Where K is the number of train data and $Y_l^{\exp}$, Y_l^{pre} denote the experimental and predicted values for train data, respectively. Several error back propagate-based iterations (epochs) are required to gain the optimized values of weights and biases. It is very important to note that the number of epochs should not lead to overtrain or undertrain problems for model [25]. Model's undertrain leads to lack of complete learning of model and in the case of overtrain the model just memorizes and does not learn, which both lead to ineffective performance of network.

2.2. Radial Basis Function Neural Network (RBF-ANN)

Radial basis function networks are feed forward networks which their hidden layer uses a radial basis function as activation function. RBF networks approximate any function by using radially symmetric and local functions [26–28]. Fig. 3 shows the architecture of these networks. Generally RBFNs have three layers in their structure which are input, hidden, and output layers. Usually the hidden layer includes the Gaussian function and a sigmoid or linear function is located in output layer. The training process in RBFNs is faster than other feed forward neural networks. RBFNs have several features such as ability of online learning, good generalization capability and great ability in controlling input noises [25,29,30]. Considering the good generalization of RBFNs, they could react and respond to unseen patterns of data very well [31]. The architecture of RBFNs is similar to classical regularization networks. The regularization networks usually have three features which are [25,32,33]:

(1) Any multivariable continuous function could be approximated appropriately by these networks in the presence of enough units.
(2) The solution is always the best possible solution because it minimizes a cost function which controls the extent of its oscillation.
(3) The prediction of network is optimal in the sense that it uses linear unknown coefficients.
(4) Another difference between RBF and MLP networks is in the classification methods of networks. In RBF hyper spheres are used to discriminate the clusters, while in MLP networks classification of clusters is attributed to hyper surfaces.

In RBF networks the input parameters which are in the form of a single input vector undergo a nonlinear transformation in hidden layer, this means that the RBF activation function in hidden layer serve as network neuron. Before applying nonlinear transformation by RBF activation function, the input variables should be multiplied by related bias terms. A vector which is the distance between the multiplied inputs and their related weights serves as the input of RBF activation function. The output layer which serves as a nonlinear combiner maps the nonlinearity into a new domain [25,29,34]. The network output for an input pattern such as x could be expressed as below:

$$y_i(x) = \sum_{k=1}^{J_2} w_{ki}\phi(\|x - c_k\|) \text{for } i = 1,\ldots,\mathrm{J}_3 \tag{7}$$

In above equation y_i (x) represents the ith output of RBF, w_{ik} is the weight that links the kth hidden component to ith output component and the $\|\,.\,\|$ is the Euclidean norm. The RBF $\phi(\bullet)$ represents the Gaussian function [34]. The matrix form of Eq. (7) when considering N $\{(x_k, y_k)\}$ patterns is:

$$Y = W^T\Phi \tag{8}$$

Where $W = [w_1,\ldots,w_{j_3}]$ is a weight matrix with $\mathrm{J}_2 \times \mathrm{J}_3$ dimension, $w_i = (w_{1i},\ldots,w_{j_2 i})^{\mathrm{T}}$, $\Phi = [\phi_1,\ldots,\phi_N]$ is matrix with $\mathrm{J}_2 \times N$ dimension, $\phi_p = (\phi_{p1},\ldots,\phi_{pJ_2})^T$ is the pth pattern of output layer, $\phi_{pk} = \phi(\|x_p - c_k\|)$, $Y = [y_1,\ldots,y_N]$ is a $\mathrm{J}_3 \times N$ matrix and $y_p = (y_{p1},\ldots,y_{pJ_3})^T$.

RBF network can approximate continuous functions with an acceptable accuracy when the RBF is suitably chosen [32,35,36]. The Gaussian RBFN is capable to predict any continuous function by using a standard deviation $\sigma > 0$ in the presence of enough number of centers c_i, $i = 1,\ldots,\mathrm{J}_2$ in the L_p-norm, $p \in [1,\infty]$ [37]. Similar to MLP the cost function which controls the optimum criterion in the training phase is minimization of MSE Eq. (6). The RBF weights and corresponding biases are necessary parameters during the training process. The accuracy and quality of developed RBF model depends greatly on the proper selection of RBF centers. These centers could be specified randomly or by categorization or using an online learning method. Another method is to use the k-NN classification scheme which initially choses the whole set of data points as desired centers and after that eliminates several of them [38]. Various kinds of RBFs are commonly used

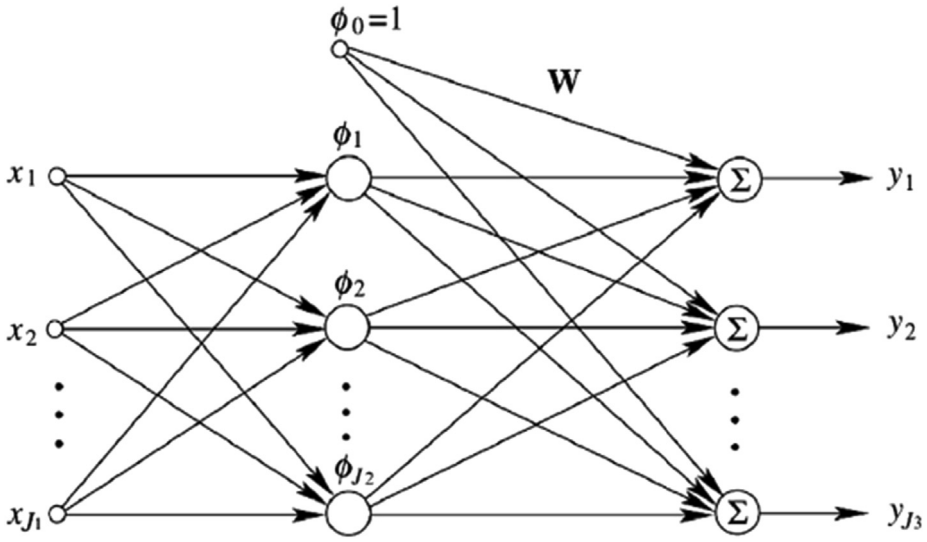

Fig. 3. Schematic representation of RBFN [29].

which the Gaussian function is the most used and popular [31]:

$$\phi(r) = e^{-\frac{r^2}{2\sigma^2}} \quad (9)$$

Where r which is a positive value denotes the distance between a data such as x and a center c, σ is a parameter which evaluates the homogeneity of regression function.

3. Result and discussion

3.1. Data acquisition

It is very important to use accurate and valid data, which cover a wide range of parameters for developing a precise and dependable model [25]. In this study 173 data points from a published work [12] was used to develop the RBF and MLP intelligent models. The TEG concentrations (wt %) and temperatures (T) data were used as the input parameters of the two proposed models and the equilibrium dew point temperature of water (T_d) was the output parameter. Details of input and output parameters are utilized in Table 1.

3.2. Model development

First, the 173 data points were divided into two subsets. About 80% of data points (138 data point) were used as training data to train the RBF and MLP models. The rest 20% (35 data points) of data were used for validation and testing of models. For MLP model the back propagation algorithm was used to optimize the values of weights and biases. As it mentioned before, a MLP network could have one or several hidden layers in its structure. It was mathematically proved that ANN is capable to effectively predict every function by using only one hidden layer [39]. Hence for the purpose of minimize the period of modeling process and saving time; in this study just MLPs which their structure contain only one hidden layer and different number of neurons were utilized. In developed MLP two neurons were located in input layer because of two input parameters and one neuron was attributed to output layer. The performance of MLP networks was examined by changing number of neurons which are located in hidden layer from 4 to 25. The values of MSE versus hidden layer located neurons for different MLPs are shown in Fig. 4. In Fig. 4 the vertical axis is the calculated MSE between experimental data and the model outputs and the horizontal axis denotes the number of neurons which were include in hidden layer. As is clear from this figure the MLP network in which 18 neurons are located in its hidden layer gives the lowest value of MSE. Thus, the MLP that 18 neurons are located in its hidden layer exhibits the best performance. The transfer function used for hidden layer was a log-sigmoid function represented by Eq. (3).

Table 1
Details of input and output data.

Parameter	Min.	Max.	Average	Standard deviation
Temperature (°C)	10	75	39.84	19.38
TEG concentration (%)	90	99.997	98.92	2.22
Equilibrium dew point temperature (°C)	−78	20	−31.39	25.93

3.3. Accuracy of the proposed model and validation

The accuracy of model was investigated by statistic and graphic approaches. Fig. 5 and Fig. 6 show the experimental data versus predicted data based on RBF and MLP and models, respectively. According to these figures the results obtained by MLP model is excellent because the 45° line and the best fitting line extremely overlap and cover each other. The correlation coefficient of both models were greater than 0.9 (0.9998 for MLP and 0.9918 for RBF) but the results of MLP model are much favorable and closer to experimental

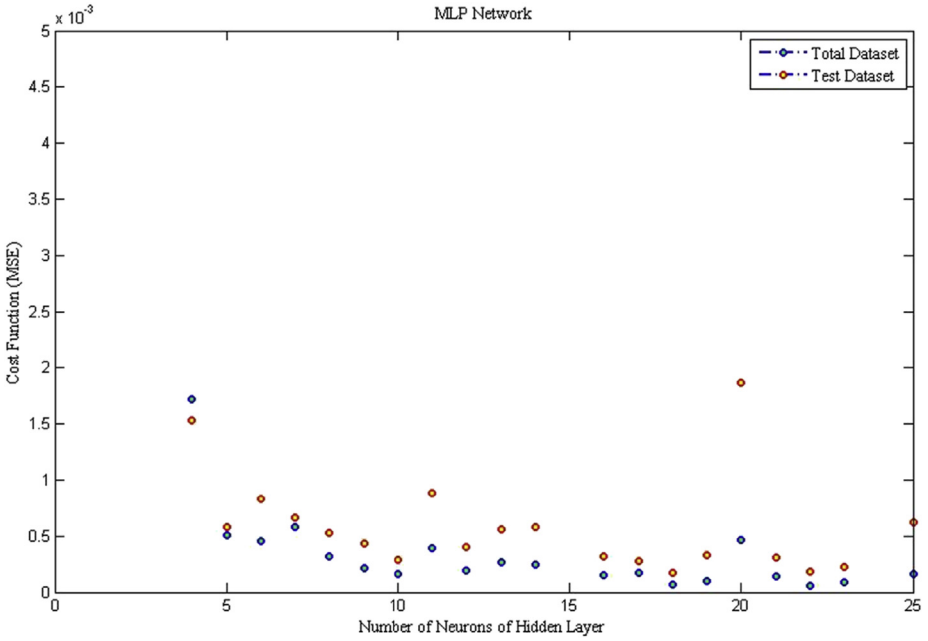

Fig. 4. Performance of different MLP networks. The horizontal and vertical axes denote number of neurons in the hidden layer and the MSE as the cost function, respectively.

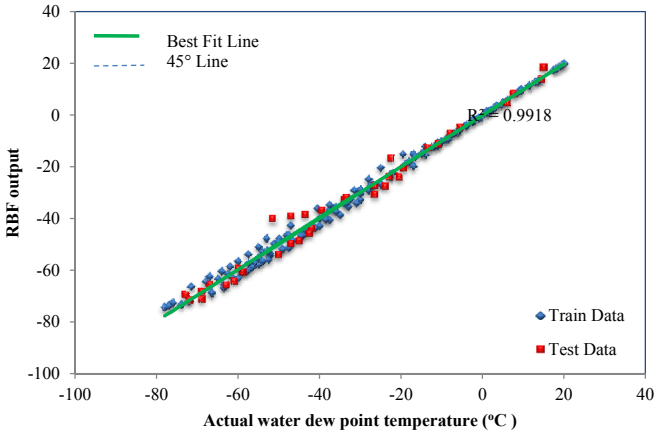

Fig. 5. Regression plots of the RBF model.

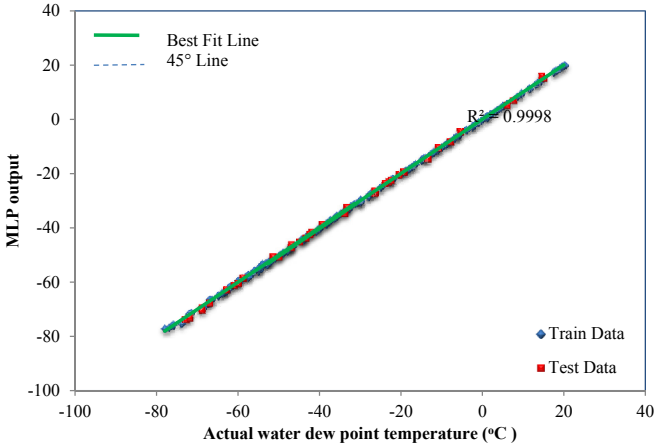

Fig. 6. Regression plots of the MLP model.

values due to higher correlation coefficient. This means that the MLP model is more precise and superior than RBF model. Fig. 7 and Fig. 8 show the relative deviation of predicted data by RBF and MLP models versus actual values of T_d. It can be seen from Fig. 7 that in the case of eliminating one data point the relative deviations of this model are between −0.3% and 0.3% which indicates the accuracy of model. There is a great consistency between the experimental values of T_d and estimated values by MLP model because as it is clear from Fig. 8, a vast number of data collapse in the interval in which the relative deviations are between −0.05% and 0.05%. Four different statistical parameters of correlation factor (R^2), Average Absolute Relative Deviation (*AARD*), Standard Deviation (*STD*), and Root Mean Squared Error (*RMSE*) are utilized Eqs. (10–13) to investigate the accuracy of the proposed models. The formulation of these parameters is as follows:

$$R^2 = 1 - \frac{\sum_{i=1}^{N}\left(\lambda_{Pred}(i) - \lambda_{Exp}(i)\right)^2}{\sum_{i=1}^{N}\left(\lambda_{Pred}(i) - \overline{\lambda}_{Exp}\right)^2} \tag{10}$$

$$\%AARD = \frac{100}{N}\sum_{i=1}^{N}\frac{\left(\lambda_{Pred}(i) - \lambda_{Exp}(i)\right)}{\lambda_{Exp}(i)} \tag{11}$$

$$RMSE = \left(\frac{\sum_{i=1}^{N}\left(\lambda_{Pred}(i) - \lambda_{Exp}(i)\right)^2}{N}\right)^{0.5} \tag{12}$$

$$STD = \sum_{i=1}^{N}\left(\frac{\left(\lambda_{Pred}(i) - \overline{\lambda}_{Exp}(i)\right)^2}{N}\right)^{0.5} \tag{13}$$

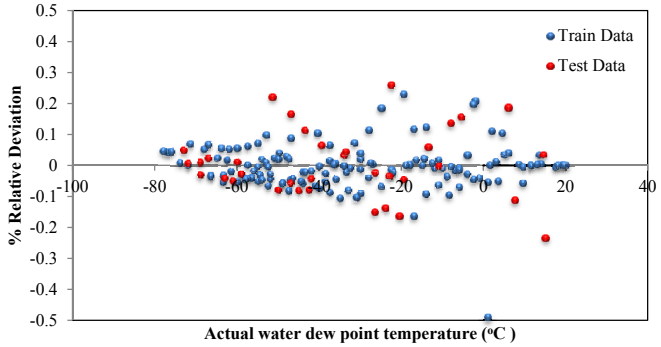

Fig. 7. Relative error deviation between real and predicted data for the RBF model.

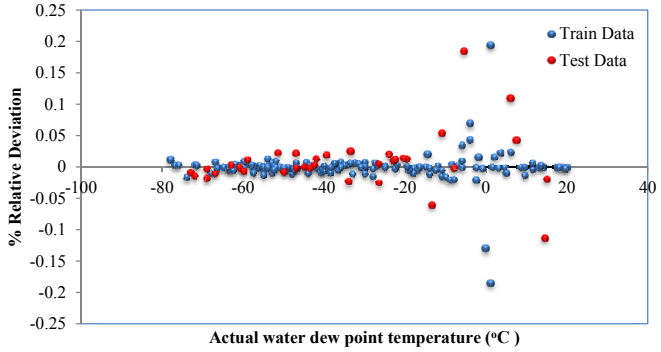

Fig. 8. Relative error deviation between real and predicted data for the MLP model.

The values of these parameters for train, test, and total dataset for two models are represented in Table 2. According to this table, the values of R^2, *AARD, STD* and *RMSE* for all data by MLP model are 0.9998, 1.29905, 0.03205, and 0.37185, respectively. However, these parameters for RBF model are 0.99176, 6.44429, 0.15707, and 2.34842, which shows that the results of MLP model are more accurate and precise than RBF model due to higher R^2 value and lower *AARD, STD* and *RMSE* values. In addition, the results of proposed models were compared with previously published models by Ahmadi et al. [1] and the results are summarized in Fig. 9 and Table 3. According to Fig. 9 and Table 3 it could be concluded that the MLP model is accurate and superior in comparison with the RBF model and the PSO-ANN and BP-ANN models, which were proposed by Ahmadi et al. [1].

Table 2
Statistical parameters of proposed models.

		R^2	*AARD*	*STD*	*RMSE*	*N*
MLP	Train data	0.999906	0.975468	0.027532	0.251843	138
	Test data	0.999399	2.574871	0.045707	0.657565	35
	All data	0.999796	1.299046	0.032049	0.371579	173
RBF	Train data	0.99413	5.92938	0.16682	1.99009	138
	Test data	0.98191	8.47449	0.11087	3.41244	35
	All data	0.99176	6.44429	0.15707	2.34842	173

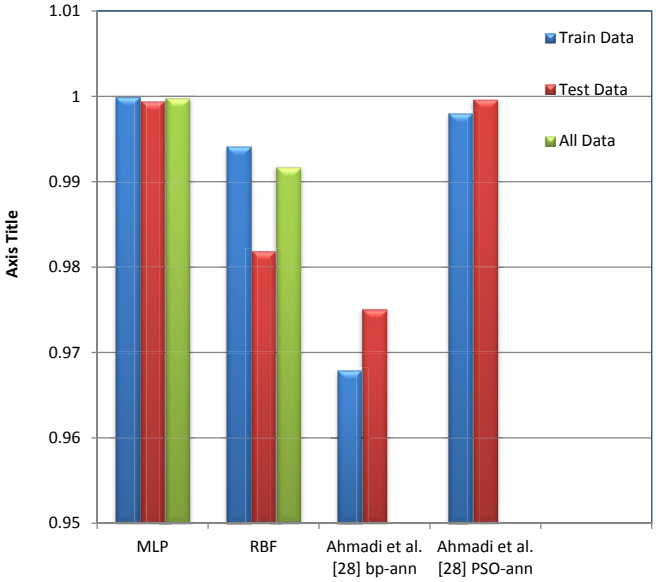

Fig. 9. Comparison between R^2 values of proposed models in this study and Models developed by Ahmadi et al. [1].

Table 3
Comparison between R^2 values of proposed models in this study and Models developed by Ahmadi et al. [1].

		R^2	*N*
MLP	Train data	0.999906	138
	Test data	0.999399	35
	All data	0.999796	173
RBF	Train data	0.99413	138
	Test data	0.98191	35
	All data	0.99176	173
PSO-ANN [1]	Train data	0.998	130
	Test data	0.9996	44
	All data	Not Available	
BP-ANN [1]	Train data	0.9679	130
	Test data	0.9751	44
	All data	Not Available	

4. Conclusion

1. The accuracy of the two proposed models in this study, namely MLP and RBF for prediction of experimental T_d values as a function of TEG concentration and contractor temperature was examined based on literature database. The results showed that the developed models could reproduce the experimental data with an acceptable accuracy based on statistical quality measure parameters such as R^2, *AARD, STD* and *RMSE*.
2. According to both graphical and statistical methods the MLP model performs much better than the RBF model in prediction of equilibrium water due point data.
3. The comparison between proposed models in this study and the model developed by Ahmadi et al. [1] showed the superiority of MLP model, which is implemented in this study.

References

[1] Ahmadi MA, Soleimani R, Bahadori A. A computational intelligence scheme for prediction equilibrium water dew point of natural gas in TEG dehydration systems. Fuel 2014;137:145−54.

[2] Ahmadi MA, Bahadori A. Prediction performance of natural gas dehydration units for water removal efficiency using a least-square support vector machine. Int J Ambient Energy 2016;37:486−94.

[3] N.G.P.S. Association, G.P.S. Association, G.P. Association. Engineering data book. Suppliers Association; 1957.

[4] Bahadori A. New model predicts solubility in glycols. Oil Gas J 2007;105:50.

[5] Bahadori A. New model calculates solubility of light alkanes in triethylene gycol. Pet Chem 2009;49:171−9.

[6] Bahadori A, Hajizadeh Y, Vuthaluru H, Tade M, Mokhatab S. Novel approaches for the prediction of density of glycol solutions. J Nat Gas Chem. 2008;17:298−302.

[7] Parrish WR, Won K, Baltatu M. Phase behavior of the triethylene glycol-water system and dehydration/regeneration design for extremely low dew point requirements. In: Proceedings of the 65th Annual GPA Convention, San Antonio, TX; 1986. p. 10−2.

[8] Herskowitz M, Gottlieb M. Vapor-liquid equilibrium in aqueous solutions of various glycols and polyethylene glycols. 1. Triethylene glycol. J Chem Eng Data 1984;29:173−5.

[9] Rosman, A. Water equilibrium in the dehydration of natural gas with triethylene glycol.

[10] Bestani B, Shing KS. Infinite-dilution activity coefficients of water in TEG, PEG, glycerol and their mixtures in the temperature range 50 to 140 °C. Fluid Phase Equilibria 1989;50:209−21.

[11] Scauzillo, F.R. Equilibrium ratios of water in the water-triethylene glycol-natural gas system.

[12] Bahadori A, Vuthaluru HB. Rapid estimation of equilibrium water dew point of natural gas in TEG dehydration systems. J Nat Gas Sci Eng 2009;1:68−71.

[13] Twu CH, Tassone V, Sim WD, Watanasiri S. Advanced equation of state method for modeling TEG−water for glycol gas dehydration. Fluid Phase Equilibria 2005;228−229:213−21.

[14] Twu CH, Sim WD, Tassone V. A versatile liquid activity model for SRK, PR and a new cubic equation-of-state TST. Fluid Phase Equilibria 2002;194−197:385−99.

[15] Talebi R, Ghiasi MM, Talebi H, Mohammadyian M, Zendehboudi S, Arabloo M, et al. Application of soft computing approaches for modeling saturation pressure of reservoir oils. J Nat Gas Sci Eng 2014;20:8−15.

[16] Zendehboudi S, Shafiei A, Bahadori A, James LA, Elkamel A, Lohi A. Asphaltene precipitation and deposition in oil reservoirs−Technical aspects, experimental and hybrid neural network predictive tools. Chem Eng Res Des 2014;92:857−75.

[17] Ghiasi MM, Bahadori A, Zendehboudi S, Jamili A, Rezaei-Gomari S. Novel methods predict equilibrium vapor methanol content during gas hydrate inhibition. J Nat Gas Sci Eng 2013;15:69−75.

[18] Kamari A, Arabloo M, Shokrollahi A, Gharagheizi F, Mohammadi AH. Rapid method to estimate the minimum miscibility pressure (MMP) in live reservoir oil systems during CO2 flooding. Fuel 2015;153:310−9.

[19] Kamari A, Bahadori A, Mohammadi AH, Zendehboudi S. Evaluating the unloading gradient pressure in continuous gas-lift systems during petroleum production operations. Petrol Sci Technol 2014;32:2961−8.

[20] Nouri-Taleghani M, Mahmoudifar M, Shokrollahi A, Tatar A, Karimi-Khaledi M. Fracture density determination using a novel hybrid computational scheme: a case study on an Iranian Marun oil field reservoir. J Geophys Eng 2015;12:188.

[21] Tatar A, Shokrollahi A, Halali MA, Azari V, Safari H. A hybrid intelligent computational scheme for determination of refractive index of crude oil using SARA fraction analysis. Can J Chem Eng 2015;93:1547−55.

[22] Shokrollahi A, Tatar A, Safari H. On accurate determination of PVT properties in crude oil systems: Committee machine intelligent system modeling approach. J Taiwan Inst Chem Eng 2015;55:17−26.

[23] Scarselli F, Chung Tsoi A. Universal approximation using feedforward neural networks: a survey of some existing methods, and some new results. Neural Netw 1998;11:15−37.

[24] Hykin S. Neural networks: a comprehensive foundation. New Jersey: Printice-Hall. Inc.; 1999.

[25] Tatar A, Yassin MR, Rezaee M, Aghajafari AH, Shokrollahi A. Applying a robust solution based on expert systems and GA evolutionary algorithm for prognosticating residual gas saturation in water drive gas reservoirs. J Nat Gas Sci Eng 2014;21:79−94.

[26] Sermpinis G, Theofilatos K, Karathanasopoulos A, Georgopoulos EF, Dunis C. Forecasting foreign exchange rates with adaptive neural networks using radial-basis functions and Particle Swarm Optimization. Eur J Oper Res 2013;225:528−40.

[27] Chen S-A, Ou Y-Y, Lee T-Y, Gromiha MM. Prediction of transporter targets using efficient RBF networks with PSSM profiles and biochemical properties. Bioinformatics 2011;27:2062−7.

[28] Ou Y-Y, Gromiha MM, Chen S-A, Suwa M. TMBETADISC-RBF: Discrimination of -barrel membrane proteins using RBF networks and PSSM profiles. Comput Biol Chem 2008;32:227−31.

[29] Tatar A, Shokrollahi A, Mesbah M, Rashid S, Arabloo M, Bahadori A. Implementing Radial Basis Function Networks for modeling CO2-reservoir oil minimum miscibility pressure. J Nat Gas Sci Eng 2013;15:82−92.

[30] Santos RB, Rupp M, Bonzi SJ, Fileti AMF. Comparison Between Multilayer Feedforward Neural Networks and a Radial Basis Function Network to Detect and Locate Leaks in Pipelines Transporting Gas. Chem Eng Trans 2013;32:1375−80.

[31] Hao Y, Tiantian X, Paszczynski S, Wilamowski BM. Advantages of radial basis function networks for dynamic system design. IEEE Trans Ind Electron 2011;58:5438−50.

[32] Poggio T, Girosi F. Networks for approximation and learning. Proc IEEE 1990;78:1481−97.

[33] Girosi F, Poggio T. Networks and the best approximation property. Biol. Cybern. 1990;63:169−76.

[34] Du K-L, Swamy MNS. Radial basis function networks, neural networks in a softcomputing framework. London: Springer; 2006. p. 251−94.

[35] Liao Y, Fang S-C, Nuttle HLW. Relaxed conditions for radial-basis function networks to be universal approximators. Neural Netw 2003;16:1019−28.

[36] Shan O, Zheng B. Fast principal component extraction by a weighted information criterion. IEEE Trans Signal Process 2002;50:1994−2002.

[37] Park J, Sandberg IW. Universal Approximation Using Radial-Basis-Function Networks. Neural Comput 1991;3:246−57.

[38] Devijver PA, Kittler J. Pattern recognition: a statistical approach. Englewood Cliffs, N.J: Prentice/Hall International; 1982.

[39] Cybenko G. Approximation by superpositions of a sigmoidal function. Math Control Signal Syst 1989;2:303−14.